The British Journal of Radiology, 83 (2010), 344–350

SHORT COMMUNICATION

Dual-energy contrast-enhanced digital breast tomosynthesis – a feasibility study

A-K CARTON, PhD, S C GAVENONIS, MD, J A CURRIVAN, E F CONANT, MD, M D SCHNALL, MD, PhD and A D A MAIDMENT, PhD

Hospital of the University of Pennsylvania, Department of Radiology, 1 Silverstein, 3400 Spruce Street, Philadelphia, PA 19104, USA

ABSTRACT. Contrast-enhanced digital breast tomosynthesis (CE-DBT) is a novel modality for imaging breast lesion morphology and vascularity. The purpose of this study is to assess the feasibility of dual-energy subtraction as a technique for CE-DBT (a temporal subtraction CE-DBT technique has been described previously). As CE-DBT evolves, exploration of alternative image acquisition techniques will contribute to its optimisation. Evaluation of dual-energy CE-DBT was conducted with Institutional Review Board (IRB) approval from our institution and in compliance with federal Health Insurance Portability and Accountability Act (HIPAA) guidelines. A 55-year old patient with a known malignancy in the right breast underwent imaging with MRI and CE-DBT. CE-DBT was performed in the medial lateral oblique view with a DBT system, which was modified under IRB approval to allow high-energy image acquisition with a 0.25 mm Cu filter. Image acquisition occurred via both temporal and dual-energy subtraction CE-DBT. Between the pre- and post-contrast DBT image sets, a single bolus of iodinated contrast agent (1.0 ml kg^{-1}) was administered, followed by a 60 ml saline flush. The contrast agent and saline were administrated manually at a rate of $\sim$2 ml s^{-1}. Images were reconstructed using filtered-back projection and transmitted to a clinical PACS workstation. Dual-energy CE-DBT was shown to be clinically feasible. In our index case, the dual-energy technique was able to provide morphology and kinetic information about the known malignancy. This information was qualitatively concordant with that of CE-MRI. Compared with the temporal subtraction CE-DBT technique, dual-energy CE-DBT appears less susceptible to motion artefacts.

Received 20 November 2008
Revised 3 April 2009
Accepted 7 April 2009

DOI: 10.1259/bjr/80279516

Breast tumour growth and metastasis are accompanied by the development of new blood vessels that have an abnormally increased permeability [1]. As a result, the absorption of vascular contrast agents in malignant breast tissue is often different to that in benign and normal tissues. Today, contrast-enhanced MRI (CE-MRI), which uses a gadolinium chelate as a vascular contrast agent, is the standard for vascular imaging of breast cancers [2–7]. Breast lesion characterisation with CE-MRI relies on a combination of the analysis of the morphological features of the lesion and the vascular enhancement kinetics.

Preliminary studies have demonstrated that contrast-enhanced digital breast tomosynthesis (CE-DBT) using an iodinated vascular contrast agent has the potential to demonstrate morphology and vascular enhancement information concordant with that of CE-MRI [8]. As the clinical uses of CE-MRI continue to expand, investigation into a potential alternative such as CE-DBT (which is projected to be less costly and more widely available than MRI) may also increase in importance.

Address correspondence to: A-K Carton, Hospital of the University of Pennsylvania, Department of Radiology, 1 Silverstein, 3400 Spruce Street, Philadelphia, PA 19104, USA. E-mail: Ann-katherine.carton@uphs.upenn.edu

Two CE X-ray imaging techniques have been proposed: temporal and dual-energy subtraction. In temporal subtraction breast X-ray imaging, one pre-contrast and one (or more) post-contrast time-points are acquired using a spectrum predominantly above the K-edge of iodine (33.2 keV) [9–12]. Pre- and post-contrast images are then subtracted logarithmically, yielding iodine-enhanced images. In dual-energy subtraction, post-contrast images are acquired in pairs at energies that closely bracket the K-edge of iodine [13–16]. At each time point, iodine-enhanced images are calculated by weighted logarithmic subtraction of the low- and high-energy (LE and HE) images.

The objective of this study was to assess the feasibility of applying a dual-energy subtraction technique to CE-DBT. In addition, we sought to compare the quality of the images obtained with a dual-energy CE-DBT technique with those obtained via temporal subtraction CE-DBT.

Methods and materials

Eligibility criteria

IRB approval was obtained for a pilot project to assess the clinical feasibility of temporal and dual-energy

subtraction CE-DBT. The CE-DBT pilot study was part of a National Cancer Institute-funded grant (NIH P01 CA85484-01A2) evaluating multimodality breast imaging. A patient with a known malignancy (status post ultrasound-guided core biopsy with clip placement) was imaged with temporal and dual-energy subtraction CE-DBT techniques and with CE-MRI. We present the findings from this index patient.

Imaging protocol

Temporal and dual-energy subtraction CE-DBT imaging was performed with a General Electric Senographe DS DBT prototype system (GE Medical Systems, Chalfont St. Giles, UK). The system was modified under IRB approval to allow HE image acquisition by adding a 0.25 mm Cu filter (Alfa Aesar, Ward Hill, MA) to the X-ray beam path. CE-DBT was performed using a single breast compression in the mediolateral oblique view of the affected breast, with the patient remaining seated for the duration of the exam. The DBT prototype used in this study did not have the ability to record compression force; light to moderate compression was applied to immobilise the breast and to reduce the radiation dose, latitude and X-ray scatter.

The timing of the DBT image sequence is shown in Figure 1. First, a pre-contrast HE DBT projection image series was acquired. After contrast agent administration, two sets of HE and LE DBT projection series were acquired. The technical parameters for the HE and LE image series for this patient are specified in Table 1. The technique was optimised as a compromise between iodine enhancement and the patient radiation dose, in consideration of the breast thickness, the heating and cooling capacity of the X-ray tube and the time for image read-out. The optimisation procedure followed the method reported previously [17].

Each DBT projection series consists of seven images acquired in 6.7° increments over a 40° arc. The X-ray tube moved in a step-and-shoot fashion under computerised motor control. The X-ray tube was moved in the same direction for each image series, and then returned to its original start position between each series.

The contrast agent was Visipaque-320® (320 mg I ml^{-1} iodixanol; Amersham, Princeton, NJ) at a dose of 1.0 ml kg^{-1} body weight. For the index patient, 85 ml was administered, given the patient's weight (85 kg). The contrast agent injection was followed by a 60 ml saline flush. The contrast agent and saline were administrated manually at a rate of ~2 ml s^{-1} into the contralateral antecubital vein.

The total procedure time was 6 m 35 s. The HE pre-contrast series took approximately 15 s to acquire; immediately thereafter, contrast injection began. The total injection time (contrast agent + saline flush) was approximately 70 s. Ninety seconds after the start of the contrast injection, the first HE post-contrast series was acquired. The first LE post-contrast series was initiated 3 m 10 s after the start of the injection; the second post-contrast HE series occurred at 4 m 50 s after the start of the injection; and the second post-contrast LE series occurred 6 m 20 s after the start of the injection. The time delay between the post-contrast series was limited by the image read-out time of the X-ray detector.

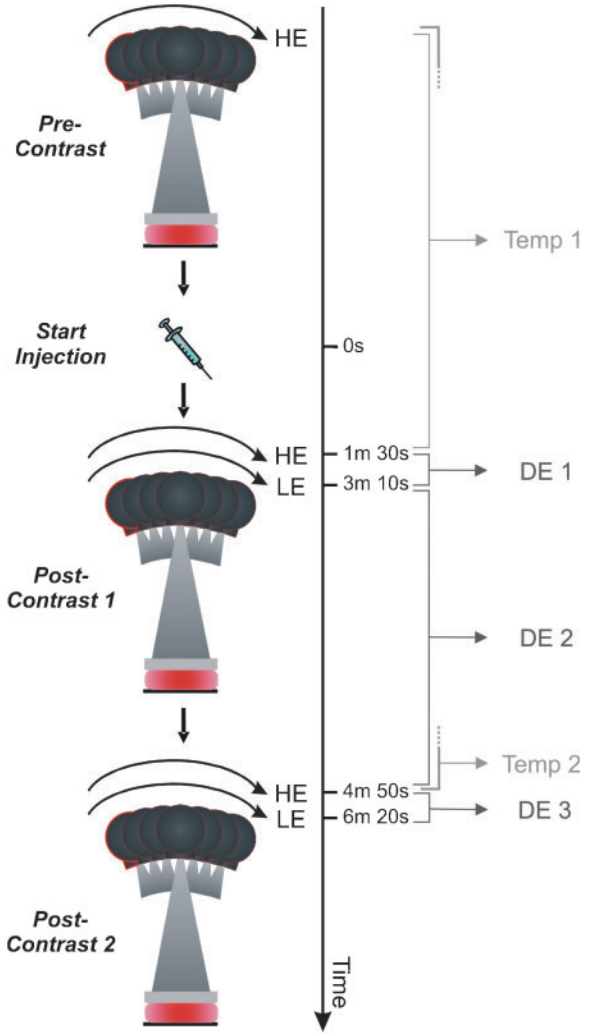

Figure 1. Illustration of the imaging sequence and timing of acquisition. The affected breast is compressed, after which a high-energy (HE) pre-contrast tomosynthesis image series is acquired. After injection, two HE/LE (low-energy) tomosynthesis image series are acquired. After image processing and tomographic reconstruction, temporal subtraction CE-DBT images at two time points (Temp 1 and Temp 2) and dual-energy (DE) contrast-enhanced digital breast tomosynthesis images at three time points (DE 1, DE 2 and DE 3) were available.

Table 1. Technical parameters used to acquire the high energy (HE) and low energy (LE) digital breast tomosynthesis projection image series. The mean glandular dose (MGD) is specified for a 5 cm thick 50%/50% glandular/adipose breast

	Target	Filter	kVp	HVL (mm Al)	mAs	MGD (mGy)
HE	Rh	25 μm Rh + 0.25 mm Cu	49	3.36	160	0.58
LE	Rh	25 μm Rh	30	0.44	71	2.37

Cu, copper; Al, aluminium; Rh, rhodium; HVL, half value layer; kVp, tube potential; mAs, current-time product.

The total mean glandular dose (MGD) was 6.5 mGy for the index patient with a breast thickness of 5 cm in compression with 50%/50% glandular/adipose tissue. By comparison, the US average MGD for two-view screening mammography in 2006 was 3.6 mGy for a reference phantom equivalent to a 4.7 cm 50/50 breast [18]; in a recent study of five digital mammography systems, the MGD varied from 2.8 mGy to 4.8 mGy for two-view screening mammography [19]. CE-DBT results in a dose approximately twice that of screening, but which is common for diagnostic imaging. The MGD was calculated using a model published by Boone [20]. This model requires knowledge of the breast entrance dose and the spectrum incident on the breast. Breast entrance doses were calculated based on air kerma measured free-in-air with a dosimeter and ion chamber (Radcal MDH1515 and Radcal 6M, Radcal Corporation, Monrovia, CA). We simulated the input spectrum necessary for this calculation using a validated extrapolation of Boone's model for HE mammographic spectra [12, 21].

Image processing

Temporal and dual-energy subtraction iodine-enhanced images were produced from the recorded projection images; the projection images were corrected for detector non-uniformity and were linear with detector dose. Temporal subtraction projection series were obtained at two time points (Figure 1). At each time point, a logarithmic subtraction was performed between the HE pre-contrast series and the respective HE post-contrast image series.

Dual-energy subtraction projection series were generated at three time points (Figure 1). At each time point, a weighted logarithmic subtraction was applied to the HE and LE image series. In this subtraction, a weighting factor, w_t, of 0.21 was applied. This value was found to cancel breast tissue optimally in a region of the breast with constant thickness [16]. A total variation (TV) noise reduction algorithm was applied to the subtracted images to reduce the noise without blurring the image [22]. Intrinsically, dual-energy subtraction images will have lower signal than temporal subtraction images, leading to the appearance of higher relative noise. Several noise reduction methods have been proposed for dual-energy subtraction [23–25].

Tomographic reconstruction

Each subtracted projection image series was reconstructed using a filtered-back projection algorithm developed in our laboratory [26]. This reconstruction algorithm was also applied to the final LE image series to provide a three-dimensional image of the breast morphology. A $20.5 \times 20.5 \times 5.0\ cm^3$ volume of interest was reconstructed in each instance; the 5.0 cm thickness of the breast was measured by the compression device and recorded in the source image DICOM (Digital Imaging and Communication in Medicine) header. The images were reconstructed in planes parallel to the detector in 1 mm increments with an in-plane voxel pitch of 220 μm. Each reconstructed image series was written using DICOM CT information object definition to the departmental picture archiving and communication system (PACS) (Centricity V2.1; GE Medical Systems, Chalfont St. Giles, UK) and research image archive (MIRC T29; Radiological Society of North America, Oak Brook, IL) [27].

Image display

The DBT and MRI images were displayed with Efilm (V1.5.3; Merge Healthcare, Milwaukee, WI) at full resolution on two 21 inch 1200×1600 greyscale monitors (Siemens SMM-21125P, Karlsruhe, Germany) in stack mode. Monitor luminance was calibrated to the DICOM GSDF using the AAPM TG18 protocol [28].

Results

The index patient in our feasibility study had undergone ultrasound-guided core biopsy of, and clip placement in, the right upper outer quadrant breast lesion, with pathology results suggesting poorly differentiated invasive ductal carcinoma. All images show consistent lesion morphology (Figures 2–4). Suspicious rim enhancement was demonstrated on both CE-DBT techniques. This enhancement was qualitatively concordant with that demonstrated on CE-MRI in the same patient (Figure 2).

Using the conspicuity of the clip placed at biopsy as an internal marker for motion in the subtraction images, the dual-energy images have less motion artefact than the temporal subtraction images (Figures 3 and 4). Reduction of motion results in superior visualisation of the internal enhancing architecture; the tumour is sharper on the dual-energy images when compared with the temporal subtraction images.

Discussion

Malignant breast lesions often have an altered microenvironment that results in neoangiogenesis [1]. This feature of their biology can differentiate them on imaging from benign breast tissue via the uptake of the intravenous contrast agent. Currently, CE-MRI and gadolinium are used to obtain breast lesion morphology and vascular enhancement information [3, 5, 6, 29]. Recently, CE-DBT has been reported to be a potential alternative method for imaging malignant breast lesion morphology and vascular enhancement patterns [8]. A temporal subtraction CE-DBT technique has been described previously [8–11]. Here, we report the application of a dual-energy subtraction CE-DBT technique.

In this feasibility study, DBT image series were obtained via the methods described. The dual-energy CE-DBT images demonstrate gross lesion morphology, as well as enhancement information. When compared with CE-MRI in the same patient, qualitatively concordant information was obtained from the dual-energy CE-DBT images.

The temporal subtraction images were obtained with time delays of 1 m 45 s and 4 m 50 s, whereas the dual-energy images were obtained with a time delay of 1 m

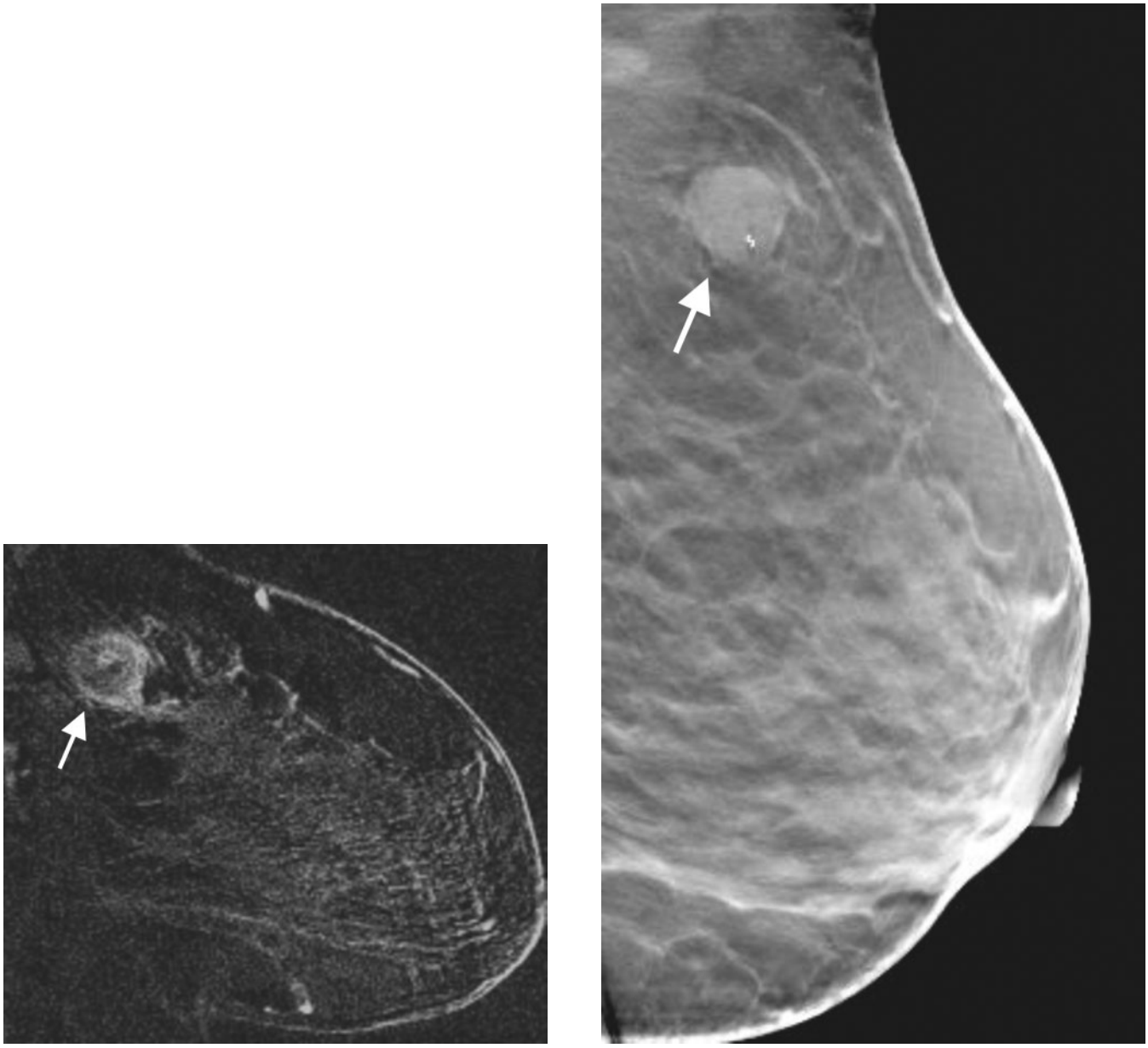

(a) (b)

Figure 2. (a) Contrast-enhanced MRI subtraction slice and (b) second post-contrast low-energy digital breast tomosynthesis slice (illustrating breast morphology) at similar planes demonstrate comparable morphological information about the malignant lesion (arrow).

40 s. When compared, less motion artefact was present on the dual-energy images. There is little difference in the motion artefact seen in the two temporal subtraction images, suggesting that the majority of the motion occurred during injection. By contrast, dual-energy images show little motion artefact because both the HE and LE images are acquired after injection. This is the practical advantage of dual-energy subtraction contrast-enhanced X-ray imaging of the breast [13–16].

Future directions

In theory, another potential advantage of dual-energy CE-DBT is that the protocol allows for a delayed post-contrast DBT pair of the contralateral breast. With a pure temporal subtraction CE-DBT technique, this contralateral imaging is not possible. As synchronous contralateral cancers do occur, information about the contralateral breast can be useful clinically.

Additional investigation into minimising motion artefacts, either *a priori* or via post-processing, is needed. This is true for both dual-energy and temporal subtraction CE-DBT techniques. For example, the dual-energy CE-DBT technique is not optimised to minimise patient motion, as the time between the acquisition of the HE and LE image series at a single time-point is 1 m 25 s. As currently implemented on our prototype instrument, this delay is necessary to allow for the read-out of each tomosynthesis projection series. Series acquisition time can be reduced by developing a dedicated CE-DBT system with rapid image read-out, where interleaved LE

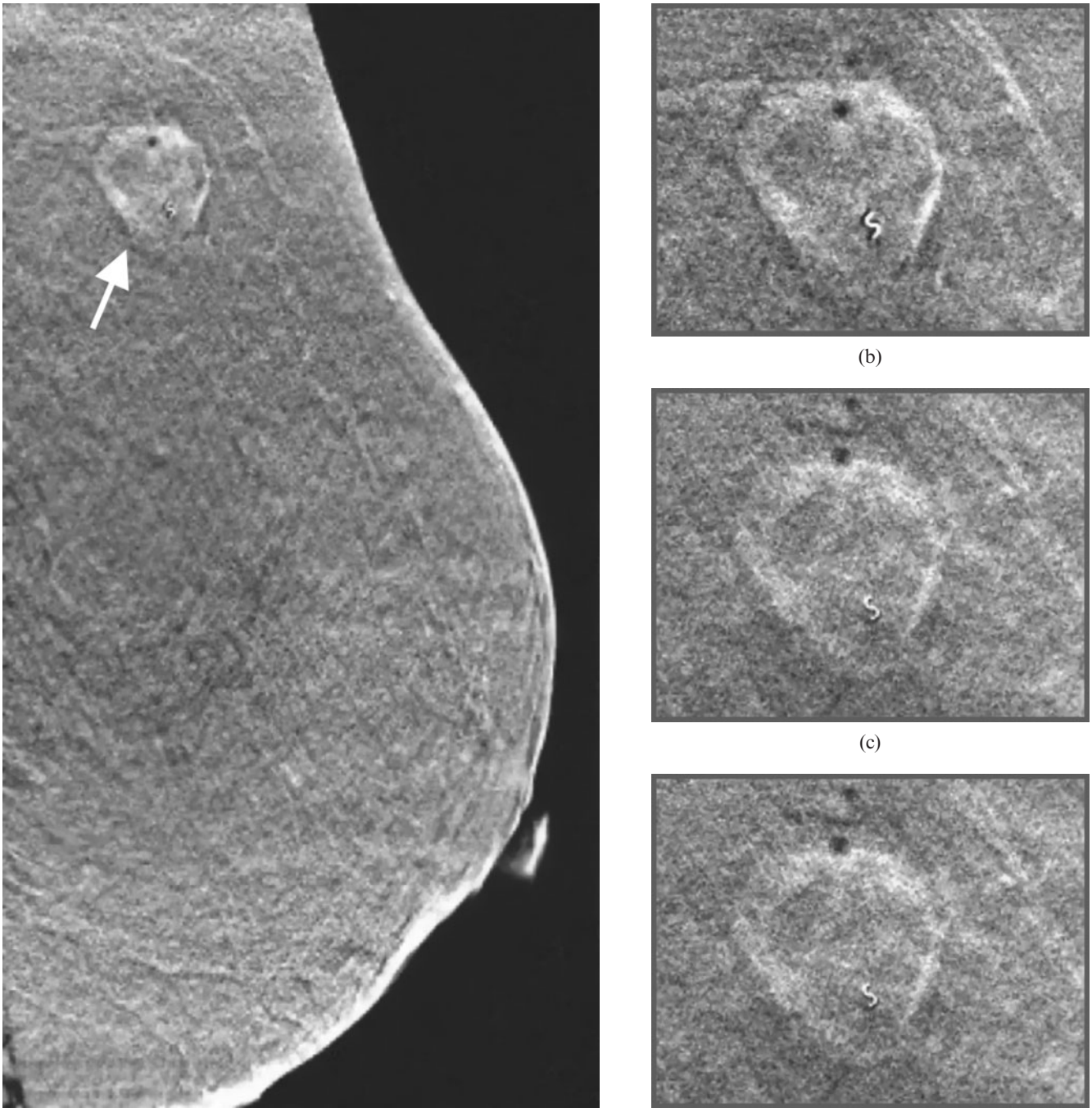

Figure 3. Dual-energy contrast-enhanced digital breast tomosynthesis image at (a) the first time point, which demonstrates the malignancy (arrow). The malignant lesion showing rim enhancement is highlighted in the zoomed images at each of the three dual-energy time points (b–d). Note that the images shown have been denoised using a TV noise reduction algorithm [22].

and HE exposures are acquired in rapid succession in one X-ray tube sweep. Decreasing the time delay between the acquisitions in dual-energy CE-DBT will not only reduce motion artefacts but also improve the temporal resolution.

Post-processing of the dual-energy CE-DBT images also requires further optimisation. With dual-energy CE-DBT, the background breast parenchyma is partially visualised even on the subtraction images. In this case, we applied a constant w_t for the compressed breast in order to cancel background breast tissue with the goal of increasing enhancement conspicuity. A breast in compression is not of a uniform thickness, however, and the optimal w_t is dependent on breast thickness [30]. Thus, to optimally cancel background breast tissue, smaller w_t values should be applied at the periphery of the breast than in the centre. Quantification of the breast thickness as a function of position at the periphery of the breast is required to fine-tune w_t. This could be achieved by incorporating a correction for X-ray field non-uniformities caused by the heel effect, beam hardening, scatter and inverse square law in the source projection images.

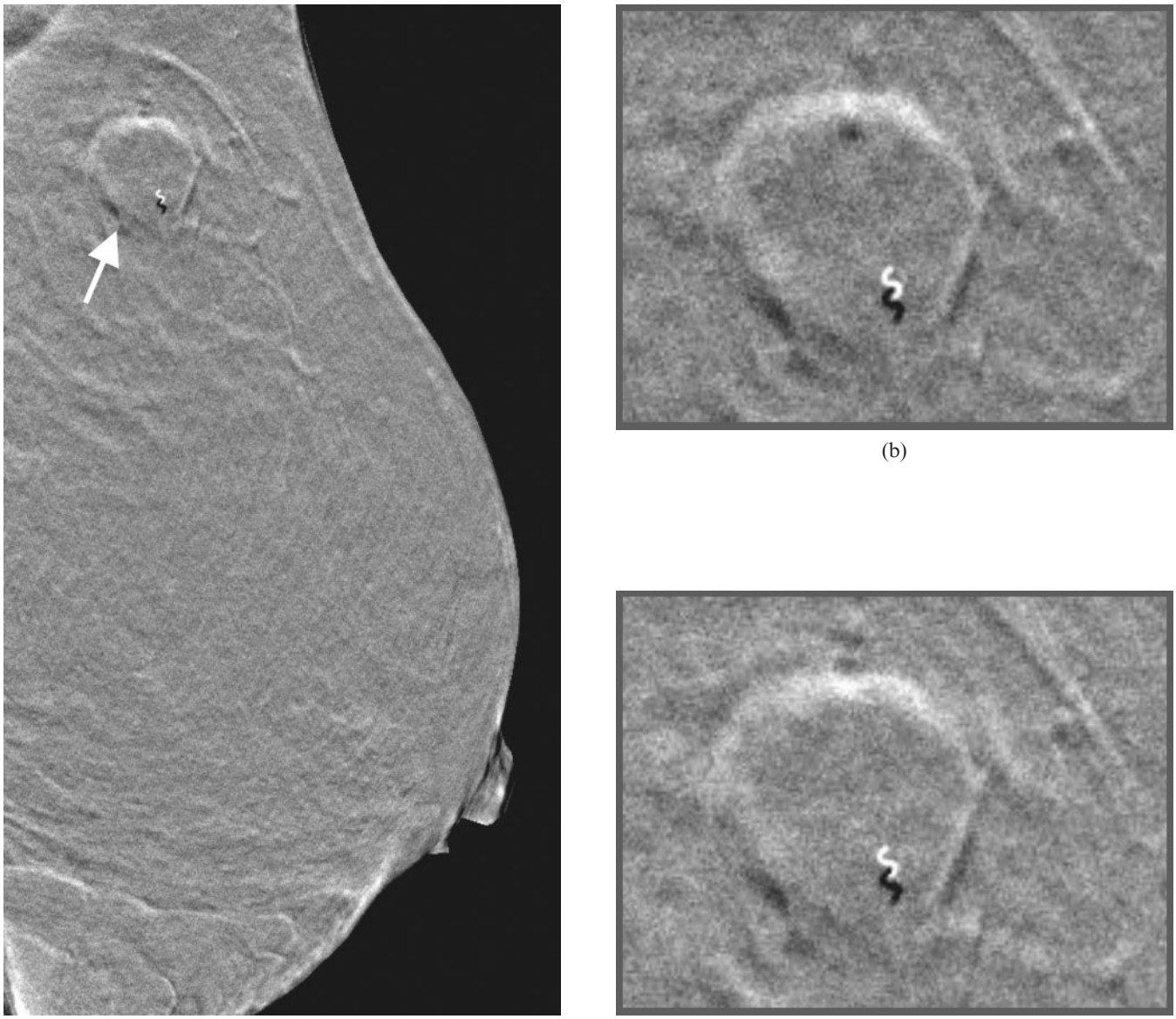

(a) (b) (c)

Figure 4. Temporal subtraction contrast-enhanced digital breast tomosynthesis (CE-DBT) image at (a) the first time point also demonstrates the malignancy (arrow). The malignant lesion showing rim enhancement is highlighted in the zoomed images at each of the two temporal subtraction time points (b,c) Note the motion artefacts in the temporal subtraction CE-DBT images; the clip in the lesion shows a displacement of approximately 2 mm.

Furthermore, power injection instead of manual injection of contrast agent should be used. With power injection, the rate of contrast administration could be doubled. Thus, the first post-contrast image series could be acquired earlier. This would potentially decrease patient motion, as well as improve temporal resolution.

Conclusions

In this study, dual-energy CE-DBT has been shown to be a clinically feasible technique. In our index patient, the dual-energy technique was able to provide information about the known malignancy with regards to its morphology and kinetics. Although this is not a clinical study, this information was qualitatively concordant with that of CE-MRI. When compared with the temporal subtraction CE-DBT technique, dual-energy CE-DBT appears less susceptible to motion artefacts. Future directions include further investigation into dual-energy CE-DBT and a comparison (or possibly fusion) of this with temporal subtraction CE-DBT.

This work was supported by a National Cancer Institute grant (NIH P01 CA85484-01A2).

References

1. Weidner N, Semple JP, Welch WR, Folkman J. Tumor angiogenesis and metastasis: correlation in invasive breast carcinoma. New England Journal of Medicine 1991;324:1–8.
2. Nunes LW, Schnall MD, Siegelman ES, Langlotz CP, Orel SG, Sullivan D, et al. Diagnostic performance characteristics of architectural features revealed by high spatial-resolution MR imaging of the breast. AJR Am J Roentgenol 1997;169:409–15.

3. Kuhl CK, Mielcareck P, Klaschik S, Leutner C, Wardelmann E, Gieseke J, et al. Dynamic breast MR imaging: Are signal intensity time course data useful for differential diagnosis of enhancing lesions? Radiology 1999;211:101–10.
4. Hylton NM. Vascularity assessment of breast lesions with gadolinium-enhanced MR imaging. MRI Clinics of North America 2001;9:321–31.
5. Nunes LW, Englander SA, Charafeddine R, Schnall MD. Optimal post-contrast timing of breast MR image acquisition for architectural feature analysis. J Magn Reson Imaging 2002;16:42–50.
6. Kuhl CK, Schild HH, Morakkabati N. Dynamic bilateral contrast-enhanced MR imaging of the breast: trade-off between spatial and temporal resolution. Radiology 2005;2005:789–800.
7. Schnall MD, Blume J, Bluemke DA, DeAngelis GA, DeBruhl N, Harms S, et al. Diagnostic architectural and dynamic features at breast MR imaging: multicenter study. Radiology 2006;238:42–53.
8. Chen SC, Carton A-K, Albert M, Conant EF, Schnall MD, Maidment ADA. Initial clinical experience with contrast-enhanced digital breast tomosynthesis. Academic Radiology 2007;14:229–38.
9. Skarpathiotakis M, Yaffe MJ, Bloomquist AK, Rico D, Muller S, Rick A, et al. Development of contrast digital mammography. Med Phys 2002;29:2419–26.
10. Ullman G, Sandborg M, Dance D, Yaffe M, Alm Carlsson G. A search for optimal x-ray spectra in iodine contrast media mammography. Phys Med Biol 2005;50:3143–52.
11. Baldelli P, Bravin A, Di Maggio C, Gennaro G, Sarnelli A, Taibi A, et al. Evaluation of the minimum iodine concentration for contrast-enhanced subtraction mammography. Phys Med Biol 2006;51:4233–51.
12. Carton A-K, Li J, Albert M, Chen S, Maidment AD. Quantification for contrast-enhanced digital breast tomosynthesis. In: Flynn MJ, Hsieh J, editors. Medical Imaging 2006: Physics of Medical Imaging. San Diego, CA, 2006:111–21.
13. Lewin JM, Isaacs PK, Vance V, Larke FJ. Dual-energy contrast-enhanced digital subtraction mammography: Feasibility. Radiology 2003;264:261–8.
14. Bornefalk H, Hemmendorff M, Hjarm T. Dual-energy imaging using a digital scanned multi-slit system for mammography: evaluation of a differential beam filtering technique. In: Flynn MJ, Hsieh J, editors. Medical Imaging 2006: Physics of Medical Imaging. San Diego, CA: SPIE, 2006: 614220-1-7.
15. Puong S, Bouchevreau X, Patoureaux F, Iordache R, Muller S. Dual-energy contrast enhanced digital mammography using a new approach for breast tissue canceling. In: Hsieh J, Flynn MJ, editors. Medical Imaging 2007: Physics of Medical Imaging. San Diego, CA: SPIE, 2007 65102H-1-12.
16. Carton AK, Lindman K, Ullberg CK, Francke T. Dual-energy subtraction for contrast enhanced digital breast tomosynthesis. In: Hsieh J, Flynn MJ, editors. Physics of Medical Imaging; 2007. San Diego, CA: SPIE, 2007 651007-1-12.
17. Carton A-K, Ullberg C, Lindman K, Francke T, Maidment ADA. Optimization of a dual-energy contrast-enhanced technique for a photon counting digital breast tomosynthesis system lecture notes in computer science. Tucson, AZ: SpringerLink, 2008:116–23.
18. Spelic DC, Kaczmarek RV, Hilohi M, Belella S. United States radiological health activities: inspection results of mammography facilities. Biomed Imaging Interv J 2007;3. www.bjr.org/2007/2/e35
19. Williams MB, Raghunathan P, More MJ, Seibert JA, Kwan A, Lo JY, et al. Optimization of exposure parameters in full field digital mammography. Med Phys 2008;35:2414–23.
20. Boone JM. Normalized glandular dose (DgN) coefficients for arbitrary x-ray spectra in mammography: computer-fit values of Monte Carlo derived data. Med Phys 2002;29:869–75.
21. Boone JM, Fewell TR, Jennings RJ. Molybdenum, rhodium, and tungsten anode spectral models using interpolating polynomials with application to mammography. Med Phys 1997;24:1863–74.
22. Total variation denoising. Available at: http://www.math.ucla.edu/~gilboa/PDE-filt/tv_denoising.html [Assessed 27 May 2009].
23. Warp RJ, Dobbins JT 3rd. Quantitative evaluation of noise reduction strategies in dual-energy imaging. Med Phys 2003;30:190–8.
24. Kalender WA, Klotz E, Kostaridou L. An algorithm for noise suppression in dual energy CT material density images. IEEE Trans Med Imaging 1988;7:218–24.
25. McCollough CH, Van Lysel MS, Peppler WW. A correlated noise reduction algorithm for dual-energy digital subtraction angiography. Med Phys 1989;16:873–80.
26. Wu T, Moore RH, Rafferty EA, Kopans DA. A comparison of reconstruction algorithms for breast tomosynthesis. Med Phys 2004;31:2636–47.
27. Medical Imaging Resource Center. Available at: http://www.rsna.org/mirc/ [Accessed 27 May 2009].
28. Samei E, Badano A, Chakraborty D, Compton K, Cornelius C, Corrigan K, et al. Assessment of Display Performance for Medical Imaging Systems, Report of the American Association of Physicists in Medicine (AAPM) Task Group 18. Med Phys 2005;32:1205–1225.
29. Nunes LW, Schnall MD, Orel SG, Hochman MG, Langlotz CP, Reynolds CA, et al. Breast MR imaging: interpretation model. Radiology 1997;202:833–41.
30. Carton A-K, Ullberg C, Lindman K, Francke T, Maidment ADA. Optimization of a dual-energy contrast-enhanced technique for a photon counting digital breast tomosynthesis system. 9th International workshop on digital mammography, 2008; Tucson, AZ: Elsevier, 2008.